

# Update for Combustion Properties of Wood Components

Mark Dietenberger\*

USDA Forest Service, Forest Products Laboratory, One Gifford Pinchot Drive, Madison, WI 53726–2398, USA  
E-mail: mdietenberger@fs.fed.us

The combustion properties of various biomass and wood materials from various references and from our laboratory were reanalysed. The net heat of combustion for cellulosic materials was found to be 13.23 kJ/g times the ratio of stoichiometric oxygen mass to fuel mass,  $r_o$ , regardless of the material composition. Bomb calorimeter data for original, charred and volatilized material components provide gross heating values, while elemental analysis of the materials for carbon, hydrogen, oxygen and ash provide direct evaluation for  $r_o$ . We corrected these data as provided in various references by converting gross heating values to lower heating values and converting elemental compositions, char fractions and  $r_o$  to a moisture-free and ash-free basis. Some existing formulae were found to disagree with data from vegetation, charred wood with high ash content, and with volatiles from cellulose treated with the fire retardant NaOH. We also established various functional correlations of  $r_o$  with elemental compositions, or volatilization fractions of untreated and treated materials, or material fractions for cellulose, lignin and extractives, or volatile fractions for tar, combustible gases and inert gases in pure nitrogen carrier gas. An interesting predictive result provides nearly constant heat of combustion while the volatile tar fraction is decreasing and combustible and inert gas fractions are increasing with time during the charring of Douglas-fir wood. Published in 2002 by John Wiley & Sons, Ltd.

## INTRODUCTION

The combustion properties of biomass and wood materials as measured in the cone calorimeter<sup>1</sup> are well known, but some puzzling characteristics make for difficult incorporation into a mathematical fire growth model. Although the surface temperature of ignition at high heat fluxes is relatively constant, it increases as the critical flux is approached or as the moisture content of wood is increased.<sup>2</sup> A sufficiently thin wood specimen will also have a lower surface ignition temperature than a thick one. The net heat of combustion property also has variations that are poorly understood. Although it is well accepted that 13.1 kJ/g is the ratio  $Dh_{c,net}/r_o$  for solid unburned clean wood, the same ratio has not been clearly verified for biomass with high ash content, treated wood, wood volatiles or wood char. By establishing the correlation in this paper, the accurate dynamic measurement of  $r_o$  in the cone calorimeter provides an effective link between the rate of heat release (RHR) and the chemistry of the specimen volatilization during flaming or char oxidation during glowing. This link to wood chemistry has not been fully exploited in the broader literature on biomass research, which we seek to remedy in this paper.

The noted features of RHR previously investigated<sup>3</sup>—the increases of peak RHR and  $Dh_c$  with imposed heat flux for wood materials—still needed elucidation by a mechanistic kinetics model. Most such models (of which there are very many) focused only on the net aggregate production of volatile components rather than considering the mathematical modelling of separate primary volatile components as a function of time and temperature. Given the rather severe experimental difficulties of characterizing the tar of wood volatilization as a function of time, we approached the problem by a complete dynamic tally of carbon, hydrogen and oxygen from a thermally thin material in a controlled heating environment. The data needed for this approach had previously been obtained by Parker and LeVan<sup>4</sup> using an instrument (named Pyrocat) with a catalytic converter and high oxygen content to ensure complete combustion of wood volatiles. The combustion products were measured with oxygen, carbon dioxide, carbon monoxide and water vapour analysers at the Forest Products Laboratory in many tests using various wood compositions. In principle, it is possible to modify the cone calorimeter to also provide the complete tally of carbon, hydrogen and oxygen in wood volatiles, which we will describe in this paper.

\*Correspondence to: M. Dietenberger, USDA Forest Service, Forest Products Laboratory, One Clifford Pinchot Drive, Madison, WI 53726-2398, USA

Previously published in Proceedings, 7th International Conference. Fire and Materials, 2001 January 22–24; San Francisco, CA. Interscience Communications: London, UK 159–171.

The use of trade or firm names is for information only and does not imply endorsement by the US Department of Agriculture of any product or service.

The Forest Products Laboratory is maintained in cooperation with the University of Wisconsin. This article was written and prepared by US Government employees on official time and is therefore in the public domain and not subject to copyright.

Other wood combustion properties such as the development of smoke (including soot and toxic gases) and gaseous products are not covered in this paper. Smoke develops from thermal cracking of volatiles and consequential incomplete combustion. One aspect of combustion we will demonstrate is thermal cracking of tar from the primary volatiles, primarily to show the constancy of heat of combustion even while the tar portion is decreasing. Smoke production data from the cone calorimeter for wood-based materials and room burn test results are compared elsewhere.<sup>5</sup>

### NET HEAT OF COMBUSTION AND STOICHIOMETRIC OXYGEN-TO-FUEL RATIO

In some standards (for example, ASTM E 1591<sup>6</sup>), net heat of combustion  $Dh_{c,net}$  is defined as the gross heat of combustion minus the latent heat of water evaporation produced from the combustion. The gross heat of combustion is measured by combustion bomb calorimetry (ASTM D 3286<sup>7</sup>). Many researchers have noted various problems in the direct use of such data for wood materials in real fire analyses, the main one being that wood chars, during which the net heat of combustion of wood volatiles is not equal to that of whole wood.<sup>4</sup> One would then resort to oxygen consumption calorimetry that uses the value 13.1 kJ/g for the heat release to oxygen consumption ratio  $Dh_{c,ox} = Dh_{c,net}/r_o$ . Assuming the specimen releases only carbon, hydrogen, oxygen and inert gases, the external oxygen supply mass fraction required for complete combustion is given by<sup>4</sup>

$$r_o = (8/3)c + 8h - o. \quad (1)$$

Huggett<sup>8</sup> and other sources indicate that research is needed to determine  $Dh_{c,ox}$  for wood volatiles, wood char, fire-retardant-treated wood and high ash content biomass. Indeed, the cone calorimeter standard<sup>1</sup> suggests using the actual value if it is available. In this respect bomb calorimetry becomes useful if one also has available ultimate analysis to determine the carbon, hydrogen, oxygen, nitrogen, sulphur and ash content of the fuel. Such data are available in the literature, some being several decades old. Some references have even used the gross heat of combustion (or alternatively

defined as the higher heating value, HHV) correlations developed for coals and extended to various biomass materials. However, it was not verified if such correlations are applicable to wood volatiles, char or treated wood. One significant collection of natural fuels data<sup>9</sup> demonstrated an approximately linear correlation of the heat of combustion at 400°C with the carbon content of the fuel. These data represent a starting point for our analysis, as gross heat of combustion and element analysis were provided for 14 different natural fuels, some with high ash content. The net heat of combustion is computed as

$$\Delta h_{c,net} = \Delta h_{c,gross} - 21.96 h \quad (2)$$

assuming the heat of water evaporation is 2.44 kJ/g. For char preparation, Susott and others<sup>9</sup> heated 1 g fuel samples (wood, stem or leaves) at 400°C for 10 min in flowing nitrogen gas. They had the original and charred samples analysed commercially for carbon and hydrogen content and obtained their gross heat of combustion and ash content from a bomb calorimeter. Because the samples had some free moisture content, they converted all measured properties to a moisture-free basis by dividing by the dried mass fraction of the unheated sample. The carbon contents of the volatiles emitted were then calculated from the equation,

$$\begin{aligned} \%C(\text{volatiles}) = \{ \%C(\text{fuel}) - \%C(\text{residue}) \\ \times (\text{fraction residue}) \} / \\ \{ 1 - \text{fraction residue} \}. \end{aligned} \quad (3)$$

Hydrogen and oxygen contents and net heat of combustion of the volatiles are computed in this paper using the same formula as for the carbon in Eqn (3). We found very few other references that have a similar type of data from which to derive combustion properties for use in Eqns (1)–(3). The data from these references as processed by Eqns (1)–(3) are presented in Fig. 1 as plots of net heat of combustion on the vertical scale and stoichiometric oxygen-to-fuel ratio on the horizontal scale. Wood materials of course have very small amounts of nitrogen and sulphur, while ash residue can be significant in certain wood species. Coal and organic waste are in the same category as the wood materials, although they have a higher aromatic content

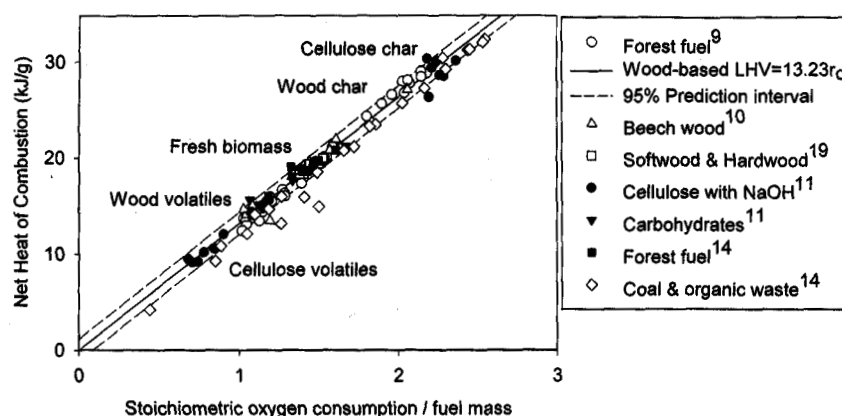


Figure 1. Correlation for net heat of combustion.

relative to the carbohydrate content, as we will see in the next section.

After ignoring coal and organic waste in Fig. 1, all data for the solid cellulosic fuels and carbohydrates (with  $r_o$  ranging from 1.2 to 1.6) are well within the 95% prediction interval with the solid line given by  $Dh_{c,ox} = 13.23$  kJ/g. In the correlation for volatiles and char, only three sources of data were found that could be included satisfactorily in the correlation. Each had somewhat different environmental conditions to vary. The oldest data obtained by Roberts<sup>10</sup> used a 10 g grounded European beech sample exposed for 1 h at temperatures ranging from 230°C to 460°C. This resulted in various levels of charring in the wood residue with  $r_o$  ranging from 1.35 to 2.05 as determined from their ultimate analysis data. They then derived the heat of combustion and carbon, hydrogen and oxygen contents for volatiles by the same formula (see Eqn (3)). From the results they concluded that the volatiles over time had a constant heat of combustion and a composition with the empirical formula,  $n(\text{CH}_2\text{O})$ , the same as the sugar monomers at  $r_o = 1.067$ . The Roberts data<sup>10</sup> are represented as upward-pointing triangles in Fig. 1 and easily fall within the 95% prediction interval of the solid line. In the next data set for a collection of forest fuels<sup>9</sup> it was found the net heat of combustion and composition of volatiles varied with the wood species, tree section and the ash content. The  $r_o$  for volatiles ranged from 1.0 to 1.3, while for the low-ash char the range for  $r_o$  is 1.8 to 2.2. The data are represented in Fig. 1 by open circles and are found approximately within the 95% prediction interval of the solid line. Of significance are two of the char samples that had ash contents of 33% and 37% corresponding to values of  $r_o = 1.49$  and 1.14, respectively. The data for these high-ash char samples are located right on the solid line in Fig. 1. The high-ash chars had added importance because they resulted in large errors calculated for the net heat of combustion when using empirical formulas originally developed for coal and organic waste. A notable result (not plotted in Fig. 1) is from Atreya<sup>2</sup>, who obtained lower heating values from the bomb calorimeter and elemental compositions of virgin wood, char and volatiles of various thick softwoods and hardwoods. However, the ash content was not considered along with the elemental compositions of C, H

and O in the analysis. If a typical ash content of 0.6% for solid wood is assumed, then a reprocessing of Atreya's data provides results agreeing with the solid line in Fig. 1, with accuracies similar to those of the forest fuels data by Sussott and others.<sup>9</sup>

The last data set<sup>11</sup> concerns the combustion properties of pure cellulose and its retardation with various levels of NaOH additive (up to 3%). Dry cylinders 2.5 cm in diameter and 5 cm in length were exposed to a radiant flux of 40 kW/m<sup>2</sup> in a chamber of flowing nitrogen gas. After a sufficiently long time (about 300 s) the researchers determined the carbon and hydrogen contents of the residue with a commercial elemental analyser. They assumed that sodium remained in the residue and used the conservation of mass to derive oxygen content. By knowing the original composition of retarded cellulose, they used a formula similar to Eqn (3) to derive the compositions of the volatiles. They also used a bomb calorimeter to determine the gross heat of combustion for the sample residue. We adopted their data with one modification: we assumed that during heating NaOH is converted to ash and water vapour, or  $\frac{1}{2}(\text{Na}_2\text{O} + \text{H}_2\text{O})$ . Then we applied Eqn (2) to their bomb calorimetry data and used Eqn (3) to determine the elemental compositions and net heat of combustion for the cellulosic volatiles. The results show a slight decrease in  $r_o = 1.185$  due to NaOH concentrations in the original samples and a relatively constant value of  $r_o = 2.2$  for the charred samples. However, the derived volatiles properties showed a wider variation in  $r_o$ , ranging from the very low value of 0.68 to a more typical value of 1.08. The data are represented in Fig. 1 as solid round circles and are on the solid line to within 95% prediction interval. All the data taken together in Fig. 1 confirmed that  $Dh_{c,ox} = 13.23$  kJ/g for cellulosic fuels in any form.

A more complete analysis results in an apparent shift of 1.23 kJ/g below the solid line in Fig. 1 for coal and organic wastes. The extended analysis also includes hydrocarbons such as methane, propane, *n*-octane and some common plastics (no oxygen content). Ultimate analysis and bomb calorimeter data for the hydrocarbons (and for carbohydrates used in Fig. 1) are taken from Heat Release in Fires,<sup>12</sup> for the coals from Mark's *Mechanical Engineer Handbook*,<sup>13</sup> and for organic waste from *Wood as an Energy Resource*.<sup>14</sup> These data are indicated in Fig. 2, where the predicted net heat of

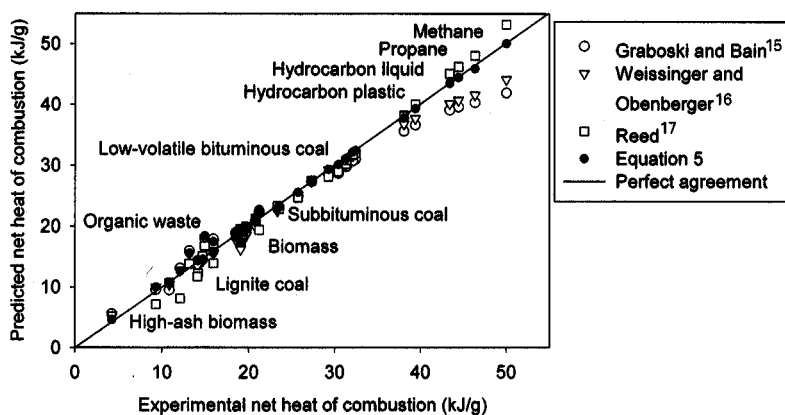


Figure 2. Comparing empirical heat of combustion to data.

combustion is plotted against the experimental net heat of combustion. Perfect correlation is the solid line. Thus to obtain the experimental net heat of combustion, Eqn (2) was applied to the measured HHV and '9.428 s' was subtracted to remove the sulphur contribution<sup>13</sup> because it was not included in the definition of Eqn (1). (We later adjust the net heat of combustion for the combustion of sulphur.) For the predicted net heat of combustion, we first consider a correlation that recognizes the difference in the heating values between biomass and coal. To correlate biomass materials, Graboski and Bain<sup>15</sup> adjusted the correlation developed for coals by a term having a linear relationship to the  $h/c$  ratio. The results of using their formula are shown as open circles in Fig. 2, which confirms the significant underpredictions for coal and hydrocarbons and good agreement for the net heat of combustion less than 30 kJ/g. Another area of disagreement (not plotted) is for the volatiles. A recent correlation<sup>16</sup> directly related the net heat of combustion with the various mass fractions of the fuel but made no adjustment for the  $h/c$  ratios. This correlation, shown as open triangles, is in close agreement for coals and organic waste but in poor agreement for fresh biomass and hydrocarbons. Another correlation<sup>17</sup> has good agreement for hydrocarbons, solid wood and coal but poor agreement for high-ash-content biomass and cellulosic volatiles. Our remedy is to first define the aromatic or aliphatic character of a fuel by removing the hydration portion of the fuel from the  $h/c$  ratio (and then using Eqn (1)) as

$$r_A \equiv \frac{h - o/8}{c} = \frac{r_o}{8c} - \frac{1}{3} \quad (4)$$

The solid circles in Fig. 2 show the best agreement ( $r^2 = 0.99$ ) using the correlation

$$\Delta h_{c,\text{net}} = 13.23r_o + 9.428s - \Delta h_{c,A} \quad (5)$$

$$\Delta h_{c,A} = 0.9 + 6r_A \quad \text{for } r_A > 0.0555$$

and

$$\Delta h_{c,A} = 0 \quad \text{for } r_A < 0.0555 = 1/18 \quad (6)$$

This formula for net heat of combustion preserves the correlation shown in Fig. 1 and provides for inclusion of organic waste/coal, ( $r_A = 0.0573$ ) and common hydrocarbons ( $r_A > 0.0555$ ). Biomass and wood products, and their charred residues, typically have  $r_A < 0.05$ . We note that certain common materials, vinyl acetate ( $r_A = 0.0417$ ,  $Dh_{c,ox} = 13.54$  kJ/g),<sup>12</sup> polycarbonate ( $r_A = 0.0417$ ,  $Dh_{c,ox} = 13.14$  kJ/g),<sup>12</sup> urea formaldehyde ( $r_A = 0.0555$ ,  $Dh_{c,ox} = 13.31$  kJ/g),<sup>12</sup> phenol ( $r_A = 0.0555$ ,  $Dh_{c,ox} = 13.05$  kJ/g)<sup>12</sup> and glycerol ( $r_A = 0.0555$ ,  $Dh_{c,ox} = 13.19$  kJ/g),<sup>12</sup> have values within 2% of  $Dh_{c,ox} = 13.23$  kJ/g. This means zeroing the aliphatic factor in Eqn (6) until  $r_A > 0.0555$ . It is noteworthy that glycerol has  $r_o = 1.216$ , a low value close to cellulose and wood volatiles. On the other hand, certain other common materials, methyl methacrylate ( $r_A = 0.0666$ ,  $Dh_{c,ox} = 12.33$  kJ/g),<sup>12</sup> polymethyl methacrylate ( $r_A = 0.0666$ ,  $Dh_{c,ox} = 12.97$  kJ/g)<sup>12</sup> and polyvinyl alcohol ( $r_A = 0.0833$ ,  $Dh_{c,ox} = 12.46$  kJ/g),<sup>12</sup> have values for net heat of combustion consistent with including the aliphatic factor in Eqns (5) and (6). A couple of exceptions to the correlation are the simplest

alcohols, *n*-propanol, ( $r_A = 0.1666$ ,  $Dh_{c,ox} = 12.81$  kJ/g),<sup>12</sup> ethanol ( $r_A = 0.1666$ ,  $Dh_{c,ox} = 12.87$  kJ/g),<sup>12</sup> methanol ( $r_A = 0.1666$ ,  $Dh_{c,ox} = 13.29$  kJ/g)<sup>12</sup> and hydrogen gas ( $r_A = \infty$ ,  $Dh_{c,ox} = 16.35$  kJ/g),<sup>12</sup> which also exist in very small quantities in the wood volatiles. Therefore, it appears that Eqns (5) and (6) have a generality beyond that of wood materials to cover many other complex materials with a closer estimate than that provided in various well-known sources.

At about  $r_A \sim 0.0555$ , there occurs an interesting discontinuous decrease in the net heat of combustion of 1.23 kJ/g, which we suspect might be the result of a change in the heat of pyrolysis at the discontinuity. We note that small endothermic heats of depolymerization and monomer evaporation combined with large exothermic heats of complete oxidation-reaction and net water condensation are measured as the higher heating value in bomb calorimetry. So if a mechanistic model of material pyrolysis calculates the heat of pyrolysis (from depolymerization and monomer evaporation), then the sum of heat of pyrolysis and lower heating value for the emitted volatile packet is the heat of complete oxidation-reaction for the volatile packet at the flame front. Unlike for some plastic materials, no reliable value for the heat of pyrolysis for wood products seems to exist. Indeed, the transient temperature profile measured within the heated charring wood showed little evidence of a heat sink (or even a heat source) beyond just that of the heat capacity in the charring region.<sup>3,4</sup> Other measurements also concluded that the heat of pyrolysis is negligible for heat transfer processes within the charring wood.<sup>18</sup> This makes the heat of complete oxidation-reaction equal to the net heat of combustion for wood volatiles.

For the case of wood materials (so that sulphur content is zero), the cone calorimeter data can be adapted to use Eqn (5) for determining the net heat of combustion and efficiency of incomplete combustion as follows. Assuming a negligible amount of total hydrocarbons during incomplete combustion, the carbon fraction of volatiles and the stoichiometric oxygen consumption per volatilized mass are obtained in the equations

$$c = \frac{12\dot{m}_{CO_2}}{44\dot{m}_f} + \frac{12\dot{m}_{CO}}{28\dot{m}_f} + \frac{\dot{m}_{soot}}{\dot{m}_f} \quad (7)$$

$$r_o = \frac{\Delta\dot{m}_{O_2}}{\dot{m}_f} + \frac{16\dot{m}_{CO}}{28\dot{m}_f} + \frac{32\dot{m}_{soot}}{12\dot{m}_f} \quad (8)$$

The mass flow rate of soot, assumed to be amorphous carbon, is derived from the laser extinction measurement of smoke using the procedure discussed by Dietenberger.<sup>5</sup> Other data available as a function of time are mass flow rates of carbon dioxide and carbon monoxide, fuel mass loss rate and observed oxygen consumption mass flow rate (see ASTM E1354<sup>1</sup>). However, one should utilize methods beyond the standard procedures to reduce the uncertainties of the terms in Eqns (7) and (8). That is, if the fuel mass loss rate is measured with a precise and quick response scale, then accurate time shifting and digital numerical deconvolution of system responses should be performed on the gas analyser signals for oxygen, carbon dioxide, carbon monoxide and soot to match the fidelity of the weigh scale signal. On the other hand, some wood

species are prone to expelling small brands, so that instead of using the weigh scale data we should obtain additional data of the water vapour flow rate to determine the fuel mass flow rate, as done with the Pyrocat data, to be explained later. The output from Eqns (7) and (8) can then be used in Eqns (4)–(6) to calculate the net heat of combustion. The effective heat of combustion as the result of incomplete combustion is computed as

$$\Delta h_{c,\text{eff}} = \Delta h_{c,\text{net}} - \frac{10.1\dot{m}_{\text{CO}}}{\dot{m}_f} - \frac{32.8\dot{m}_{\text{soot}}}{\dot{m}_f} \quad (9)$$

By substituting Eqns (5) and (8) into (9) and multiplying Eqn (9) by the mass loss rate, the true rate of heat release of a biomass fire is given by

$$\text{RHR} = 13.23\Delta\dot{m}_{\text{O}_2} - 2.54\dot{m}_{\text{CO}} + 2.48\dot{m}_{\text{soot}} \quad (10)$$

It turns out that Eqns (9) and (10) also provide accurate computations for overall heat release when carbon monoxide or soot are instead being depleted by a more complete combustion, as might occur in an afterburner (mass flow rate consumptions of carbon monoxide and soot have negative values in this case). An even more important factor is the fact that the yield of carbon monoxide and soot is typically much higher in our ISO 9705 room/corner burn tests than that in the cone calorimeter tests. All these factors also make Eqn (9) or (10) particularly suited for use in computer fire models.

The mass fractions of hydrogen and oxygen in the volatiles can also be calculated if the mass balance needs to consider only carbon, hydrogen and oxygen in the volatiles. This is done by substituting the mass balance into Eqn (1) to derive hydrogen and oxygen mass fractions as

$$h = (1 + r_o - 11c/3)/9 \quad (11)$$

$$o = (8 - r_o - 16c/3)/9 \quad (12)$$

The output from Eqns (7) and (8) is used in Eqns (11) and (12). With the availability of the mass fraction of hydrogen, one can now invert Eqn (2) to obtain the gross heat of combustion of the volatiles as a function of time. One has the information to correct the expansion factor utilized in calculating the oxygen depletion rate,  $\dot{D}\dot{m}_{\text{ox}}$  (see ASTM E 1354<sup>1</sup>). For other organic materials where the sulphur content may be important, or the aromatic content may not be ignored, one will require additional gas analysis equipment and an alternative set of equations to obtain the correct values of RHR and volatile elemental compositions.

## ELEMENTAL FRACTIONS AND STOICHIOMETRIC OXYGEN-TO-FUEL RATIO

Sometimes the ultimate analysis or detailed gas analyses of combustion products are not available or practical to use. Then a method is needed to calculate the carbon or hydrogen mass fractions of the fuel for use in the formulae. For example, in our laboratory several years ago,<sup>19</sup> a few different species of softwoods and hardwoods were tested in the bomb calorimeter. The same samples were also analysed for their holocellulose, lignin

and extractive contents. A correlation was then developed between the higher heating value (HHV) and the three wood contents. Fortunately, the holocellulose, lignin and extractive contents of the same samples as in Susott and others<sup>9</sup> were obtained by Rothermal.<sup>20</sup> We note Susott and others and Shafizadeh<sup>21</sup> had obtained elemental carbon, hydrogen and oxygen contents for holocellulose and lignin along with the forest fuel data, for which we derived values of  $r_o$  as 1.19 and 1.91, respectively, from Eqn (1). For all 14 forest samples, we derived the stoichiometric oxygen consumption to fuel ratio from their elemental contents and correlated it to wood structural contents as

$$r_o = 1.19(\text{fraction holocellulose}) + 1.91(\text{fraction lignin}) + 2.39(\text{fraction extractive}) \quad (13)$$

We note that in this context, the holocellulose includes the alpha-cellulose and hemicelluloses (mannan, xylan, pectin, xyloglucan and galactan).<sup>4,19,20</sup> The value of  $r_o$  as 2.39 for the extractives is most consistent with the terpin hydrate ( $\text{C}_{10}\text{H}_{22}\text{O}_3$ ,  $r_o = 2.358$ ), which can easily dehydrate to terpeniol, borneol, fenchyl alcohol and monoterpenes. These products form the main components of pine oil, an extractive obtained by steam distillation of pinewood.<sup>22</sup> The correlation given by Eqn (13) was extrapolated to White's data<sup>19</sup> on softwoods and hardwoods. To make further progress with White's data, we found the linear relationship,

$$c/(1-a) = \alpha + \beta r_o/(1-a), \quad (14)$$

applicable for cellulosic fuels with values  $\alpha = 0.0719$  and  $\beta = 0.314$ . This is shown in Fig. 3 for the four sources of data plotted on an ash-free basis implied by Eqn (14). These four references were particularly chosen for their complete data on volatiles, original fuel and charred fuel. The dashed line going through the circle data points represents Eqn (14), while the solid lines represent the relationship  $\alpha = 0$  and  $\beta = 3/8$  for carbohydrates. If we were to just limit our attention to the forest fuels data by Susott and others or to solid wood data by Atreya<sup>2</sup>, then the appropriate values are  $\alpha = 0.0$  and  $\beta = 0.353$ . By substituting the mass balance,  $1 = (c + h + o)/(1-a)$ , and Eqn (1) into (14), the mass fraction of hydrogen is

$$\frac{9h}{(1-a)} = \left(1 - \frac{11\alpha}{3}\right) + \left(1 - \frac{11\beta}{3}\right) \frac{r_o}{(1-a)} \quad (15)$$

which is shown in Fig. 3 as the dashed line going through the triangle data points. The dashed line for oxygen as computed from the mass balance equation is shown going through the square data points. These correlations have several implications, particularly for kinetics modelling of wood pyrolysis. For now, we see that Eqns (2), (5) and (15) are combined to derive a calculation for the net heat of combustion from the gross heat of combustion for cellulosic fuels as

$$\Delta h_{c,\text{net}} = \frac{\Delta h_{c,\text{gross}} - 2.44(1-a)(1 - 11\alpha/3)}{1 + 0.1844(1 - 11\beta/3)} \quad (16)$$

For White's data we used a typical ash content of 0.6%. By application of Eqns (13) and (16) to White's data and plotting on Fig. 1, we once again verified our net heat of combustion correlation to within 1% to 2% deviation error (sum of deviation errors is 0.4%). We then applied

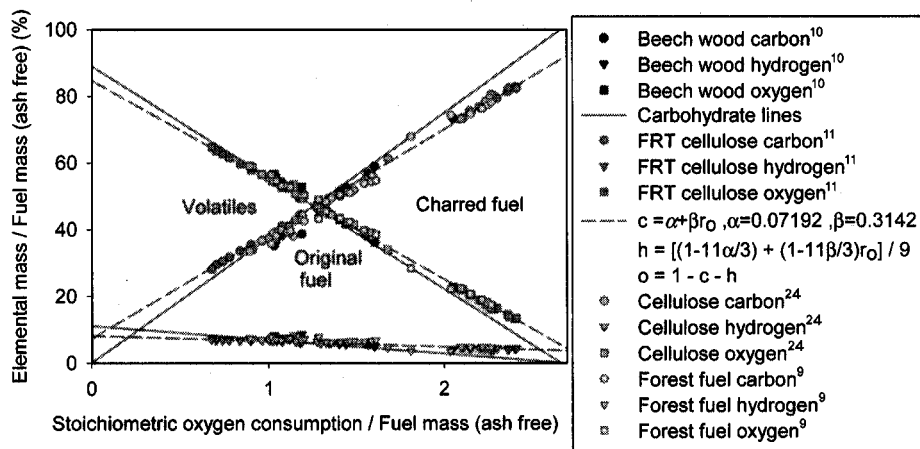


Figure 3. Correlation of elemental mass fractions.

the same steps to the coal and organic waste materials and found the coefficients to Eqn (14) as  $a=0$  and  $\beta=0.32$ . This simplified Eqn (6) to the expression  $Dh_{c,A} = 1.23 \text{ kJ/g}$ , which in turn gave the relationship

$$\Delta h_{c,net} = 1.034\{\Delta h_{c,gross} - 2.44(1 - a) + 0.0406\}. \quad (17)$$

The last group of materials is the hydrocarbons with the constants of Eqn (14) exactly as  $a = 3/2$  and  $\beta = -3/16$ . The remaining steps do not result in a simple relationship for the net heat of combustion and are not shown here. It is emphasized in this section that the solids are assumed to be fully volatilized (no residue, except for the ashes) in a single heating event, as in the bomb calorimeter or extreme flash pyrolysis. Equation (13) is not appropriate (nor even variations of it) when there is considerable charring, as Fangrat and others<sup>23</sup> have already found in their efforts at a correlation for the cone calorimeter's effective heat of combustion with wood contents. Also, we do not recommend using Eqns (16) or (17) for the cone calorimeter data, because the use of Eqns (7) to (12) should provide better results, particularly for the transient nature of volatile production during flaming.

### MECHANISTIC KINETIC ANALYSIS FOR DOUGLAS-FIR WOOD VOLATIZATION

The pyrolysis kinetics of biomass has been extensively studied by many researchers.<sup>24</sup> The main chemical events during pyrolysis are often described in the literature. Starting at temperatures of 100°C, dehydration (chemical release of water vapour leaving behind the amorphous carbon for char) accompanied by decarboxylation (release of carbon dioxide leaving behind aromatic or aliphatic char) begins to occur and then increases more rapidly around 250°C. The extractives are also vaporized within this temperature range. The hemicellulose is said to decompose first, largely between 200°C and 300°C, followed by the cellulose at 300°C to 350°C, and finally by the lignin at 280°C to 450°C.<sup>25</sup> It is presumed these decompositions are depolymerizations that release heavy monomers such as levoglucosan, glycolaldehyde, cellobiosan and anhydrosugar in various proportions. As the tempera-

ture increases under atmospheric pressure, these monomers will thermally degrade by releasing light gases such as water vapour, carbon monoxide and low-molecular-weight gaseous fuels, and do so by reducing from a heavy tar high in oxygen content to a light tar containing relatively more heavy hydrocarbons. The mechanistic kinetics analysis is very difficult to construct because the tar is very difficult to quantify experimentally and numerous gaseous molecules need to be accounted for. Difficulties with predicting net heat of combustion from a simple correlation with wood components<sup>23</sup> demonstrated a need for kinetics-type modelling to accommodate various heating regimes. One could argue that cellulose volatiles come out first with cellulose heat of combustion and then lignin volatiles come out next with lignin's heat of combustion as the reason for the very poor correlation. However, in unextracted wood the interactions of minerals and ash with cellulose and lignin gave experimental results on pyrolysis rates and heat of combustion profile that even the methods of Parker and LeVan<sup>4</sup> for kinetics of hemicelluloses, alphacellulose and lignin could not accommodate. While acknowledging these problems, it is still possible to improve upon current models.

The improvement to kinetic modelling was achieved by considering a heavy tar with the empirical formula  $C_x H_y O_z$  from depolymerization and the water vapour and carbon dioxide from the competing charring reactions. The outcome of the kinetic modelling should agree with at least three different parameters of pyrolysis having a close relationship with volatization chemistry. Other outcomes, including thermal cracking of the heavy tar to light tar, are demonstrated to show various features of the model and its robustness. To gain guidance on model development we again examine the results shown in Fig. 3 for elemental correlations. Although the correlation given by Eqns (14) and (15) actually represent properties of volatiles and char accumulated with time, their linear relationships imply that the compositions of volatiles should also follow the same correlation with similar values of  $a$  and  $\beta$  in the major part of the volatization process. This is verified in Fig. 4 using data retrieved from our laboratory Pyrocat work<sup>4</sup> on the unextracted Douglas-fir wood during the 1980s.

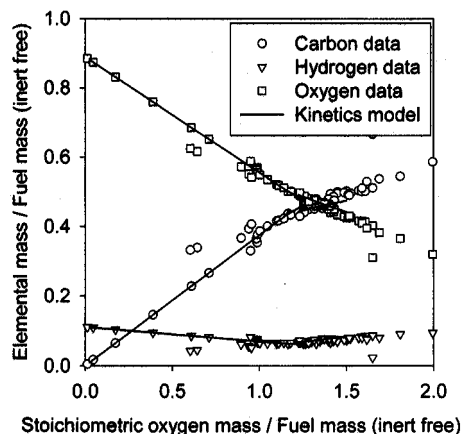


Figure 4. Elemental fractions of Douglas-fir volatiles.

The Pyrocat apparatus<sup>4</sup> provides for a complete combustion by collecting wood volatiles flow emitted from a precisely heated thin sample (typically 0.75 mm thick with a 0.25 mm thermocouple embedded in the 300 mg mass) into a nitrogen flow and passing them through enriched oxygen flow and a catalytic converter at much higher temperatures. All the C, H and O contained within the wood volatiles were then derived as a function of time from the data obtained with the gas analysers for oxygen, water vapour and carbon dioxide. The carbon monoxide analyser was used to check for the completion of combustion. The data acquisition system resulted in data collection every 5s, while the gas collection system had transit times of about 15 s and time constants of about 10s. The total pyrolysis time could be varied between 3 and 60 min (for the temperature rises to around 400°C), which was quicker than obtainable in TGA experiments but still somewhat slower than the cone calorimeter exposure, for similar specimen thickness. However, it was possible to achieve the targeted high temperatures in the specimen while only losing 10% of the mass during the steep temperature gradients. In this way, the high-temperature pathways of wood pyrolysis became observable and with better details than the 1980s-era TGA instrument. As can be seen in Fig. 4, the volatiles started out with a carbohydrate curve (where  $\alpha = 8h$ ) indicating a strong presence of water vapour. When the sample temperature nearly reached its designated equilibrium value, the data shifted its direction to look like the data trends in Fig. 3. This shift in direction can imply the presence of carbon dioxide in addition to water vapour. To better understand the significance of the results in Figs 3 and 4, consider the following volatile composition,  $C_x H_y O_z + mH_2O + nCO_2$ , and substitute in Eqn (14) (with  $a=0$ ) to solve for  $m$  and  $n$  as the formulas

$$m = \frac{X}{c_{\max}} \left( \frac{r_{\max}}{r_0} - 1 \right) / \left( \frac{3}{2} + \frac{11}{3} \frac{n}{m} \right) \quad (18)$$

$$\frac{n}{m} = \frac{9\alpha}{6 - 22\alpha} \quad (19)$$

$$c_{\max} = 12X / (12X + Y + 16Z) \quad (20)$$

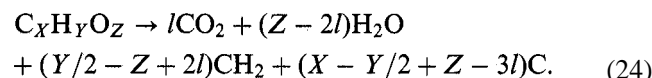
$$r_{\max} = (32X + 8Y - 16Z) / (12X + Y + 16Z). \quad (21)$$

One immediately notes that for any  $r_0 < r_{\max}$ , Eqn (19) states that the mole ratio of carbon dioxide over water vapour is a constant for the given value of  $\alpha$ . Furthermore, the mole ratio of water vapour over the volatilized monomer fuel (or tar) has an inverse proportionality to  $r_0$  given by Eqn (18). As  $r_0$  reaches  $r_{\max}$ , the tar becomes the only component of the volatile. If cellulose is the specimen, then levoglucosan,  $C_6H_{10}O_5$ , is most likely the primary monomer in the volatiles. This monomer partially changes into alpha-glucose by hydrolysing, but all of it will eventually degrade into lighter molecules as time, pressure and temperature increase. However, one can expect a progression of primary monomers from extractives, hemicelluloses, cellulose and lignin in a typical wood pyrolysis, which implies changing the  $X$ ,  $Y$  and  $Z$  as functions of time. With oxygen consumption and carbon content per fuel mass being the data readily obtainable, a rearrangement of Eqns (20) and (21) is used to estimate the hydrogen and oxygen atoms of heavy tar as a function of the carbon atoms as

$$Y = \frac{4}{3} \left( \frac{1 + r_{\max}}{c_{\max}} - \frac{11}{3} \right) X \quad (22)$$

$$Z = \frac{3}{4} \left( \frac{8 - r_{\max}}{9c_{\max}} - \frac{16}{27} \right) X. \quad (23)$$

The number of carbon atoms can be selected arbitrarily; however, the value  $X = 6$  seems to reasonably correspond to the known monomers in the primary heavy tar. For correlating with the Pyrocat data, we found it useful and simple to fix  $c_{\max}$  at a constant value (0.53 for unextracted Douglas-fir wood) while allowing,  $r_{\max} = (c_{\max} - \alpha)\beta$ , to shift to higher values to follow changes in the data trends as represented by changes in  $\alpha$  and  $\beta$ . The parameter  $\beta$  is computed as the slope of the line from the data point,  $(r_0, c)$ , to a pivot point,  $(r_{o,piv} = 1.12, c_{piv} = 3r_{o,piv}/8)$ , as seems to be suggested by Fig. 4, to give  $\beta = (c_{piv} - c) / (r_{o,piv} - r_0)$  and  $\alpha = c_{piv} - \beta r_{o,piv}$ . As our model for charring development we considered dehydration and decarboxylation acting on the monomers still not depolymerized. The empirical formula for the charring reaction (assume no oxygen is left behind) is



First we note the extreme range of charring. For low-temperature fully charred wood, there would be only dehydration. According to Eqn (24) this leads to high concentrations of amorphous carbon and low concentrations of aliphatic carbon and the volatiles containing only the water vapour. If the specimen were just cellulose, then the low-temperature charring would be fully amorphous, resulting in a reasonable ultimate char mass fraction value of 0.444. Suppose a high-temperature or a chemical treatment process makes charring a mostly decarboxylation process, then it seems reasonable that all the hydrogen is effectively trapped in long chains of aliphatic carbon. This results in high concentrations of aliphatic char and low concentrations

of amorphous char. If the specimen were just cellulose, the corresponding ultimate char mass fraction would be 0.346. More realistically, we can use Eqn (19) to estimate the mole ratio of carbon dioxide to water vapour being emitted into the wood volatiles as a result of charring, and thereby obtain an estimate for the variable  $l$  as  $Z/(2 + m/n)$ . Indeed, this transference of carbon dioxide to water vapour mole ratio along with the use of identical monomer formula as a basis for charring or volatilizing is consistent with the observation that the elemental mass fractions (C, H and O) of virgin solid, volatiles and char residue of a specimen type are located on identical linear functions in Fig. 3. For the NaOH-treated cellulose data shown in Fig. 3, Eqn (19) provides the molar ratio value  $n/m = 0.1465$ . Therefore, according to Eqn (24), for each mole of the charring cellulose monomer, the process creates 0.566 moles of carbon dioxide, 3.866 moles of water vapour, 1.133 moles of aliphatic carbon and 4.3 moles of amorphous carbon. This results in an ultimate char mass fraction value of 0.416, assuming all the cellulose monomers are charring and the water vapour and carbon dioxide are the only components of the volatiles. However, at high temperatures much of the primary monomers are evaporating, which would significantly decrease the ultimate char mass fraction and increase the heat of combustion of the volatiles. This is modelled by the following equations for volatile emission rates and char growth rates on the mass basis,

$$\dot{y}_{\text{vol}}[12X_w + Y_w + 16Z_w] = \dot{z}_b[12X + Y + 16Z] + \dot{z}_c[44l + 18(Z - 2l)] \quad (25)$$

$$\dot{y}_{\text{char}}[12X_w + Y_w + 16Z_w] = \dot{z}_c[14(Y/2 - Z + 2l) + 12(X - Y/2 + Z - 3l)] \quad (26)$$

The normalized mass loss rate,  $\dot{y}_{\text{vol}}$ , is the ratio,  $\dot{m}_f/m_w = (\dot{m}_{\text{CO}_2} + \dot{m}_{\text{H}_2\text{O}} - D\dot{m}_{\text{O}_2})/m_w$ , for the Pyrocat apparatus. The molar depolymerization rate  $\dot{z}_b$  and molar charring rate  $\dot{z}_c$  are considered to be competing for the same monomer units in the wood. The molar charring rate is in turn divided into the fraction emitting carbon dioxide and the remaining fraction emitting water vapour. Each of the molar rate components is multiplied by their molecular weights for conversion to normalized volatile mass flow rates. The normalized mass loss rate is also multiplied by the 'equivalent' molecular weight of virgin oven-dried wood to maintain consistency. The Douglas-fir wood used was measured to have 62% holocellulose, 30% lignin and 8% extractives by weight in the ash-free, moisture-free sample<sup>4</sup>. With an ash content<sup>14</sup> of 0.8%, these values are adjusted by multiplying by 0.992 and then substituted into Eqn (13) to obtain  $r_{\text{max}} = 1.49$ . According to Eqn (14), the value of  $c_{\text{max}}$  is 0.54 for cellulosic materials and 0.526 for forest fuels. These values are reasonable, considering the existing data on the commercial Douglas-fir wood.<sup>14</sup> Since the number of carbon atoms is fixed at 6, Eqns (22) and (23) are used to calculate the number of hydrogen and oxygen atoms in the virgin wood 'monomer'. We then derived the variables  $\dot{z}_b$ ,  $\dot{z}_c$ , and  $l$  uniquely from decomposing Eqn

(25) into its carbon, hydrogen and oxygen portions and solving algebraically to result in

$$\dot{z}_b = \frac{r_o(12X_w + Y_w + 16Z_w)}{8(4X + Y - 2Z)} \dot{y}_{\text{vol}}$$

$$\dot{z}_c = \left( \frac{o}{16Z} - \frac{r_o}{8(4X + Y - 2Z)} \right) \times (12X_w + Y_w + 16Z_w) \dot{y}_{\text{vol}} \quad (28)$$

$$l = \left( \frac{c(4X + Y - 2Z) - 1.5Xr_o}{o(4X + Y - 2Z) - 2Zr_o} \right) \left( \frac{4Z}{3} \right) \quad (29)$$

The values of the variables,  $r_o$ ,  $c$ ,  $o$  and  $\dot{y}_{\text{vol}}$  are derived directly from the Pyrocat data as functions of time. Because the ratio of carbon dioxide to water vapour emitted by charring is equal to the corresponding ratio in the volatiles, we combine  $n/m = l/(Z - 2l)$  with Eqn (19) to obtain the formula.

$$\frac{1}{\alpha} = \frac{3(Z - 2l)}{2l} + \frac{11}{3} \quad (30)$$

This equation can also be derived algebraically by substituting Eqns (12), (14), (20) and (21) into Eqn (29). A typical Pyrocat experiment is usually run at a long time interval to ensure complete charring of the sample. Integration of Eqn (26) with time provides the accumulated amorphous/aliphatic char production, while time integration of Eqn (25) provides the accumulated volatile production. One of the tests to verify the form of the charring reaction (Eqn (24)) is to check if the numerical integrations over the experimental run time of the sum of  $\dot{z}_b$  and  $\dot{z}_c$  is unity and that of  $\dot{y}_{\text{char}}$  is the complete char weight fraction of the sample. We found this to be true not only for the unextracted Douglas fir but also for the alpha cellulose and Kraft lignin materials tested in the Pyrocat.

Because the Pyrocat experiment includes temperature measurements within the sample using a small thermocouple, another verification is to check if the variables  $\dot{z}_b$ ,  $\dot{z}_c$  and  $l$  have viable kinetic relationships as a function of temperature only. One possible difficulty is that the normalized mass loss rate is affected by the 10 s time constant of the gas collection system, while various mass ratios (that is,  $r_o$ ,  $c$ ,  $o$ ) have complex relationships to the time constant. It is also possible the thermocouple responds with a time constant smaller than 10 s. Ideally, one would characterize the time response of each measuring component, obtain the data at short time intervals, and perform digital numerical deconvolution on each of the signals to obtain their true value. With our modern cone calorimeter data it is possible to do this data processing, but the Pyrocat apparatus was disassembled several years ago. Thus, to use the existing data, we will provisionally overlook the situation of somewhat differing time constants of various measurements. At this point we borrow Broido's<sup>26</sup> basic idea of kinetic analysis to plot the three ratios,  $\dot{z}_b/(1 - z_b - z_c)$ ,  $\dot{z}_b/\dot{z}_c$  and  $l/(Z - 2l)$  as functions of absolute temperature inverse. Figures 5–7 show the results. It became clear there were three regions of temperature intervals in which to derive the correlations. The first

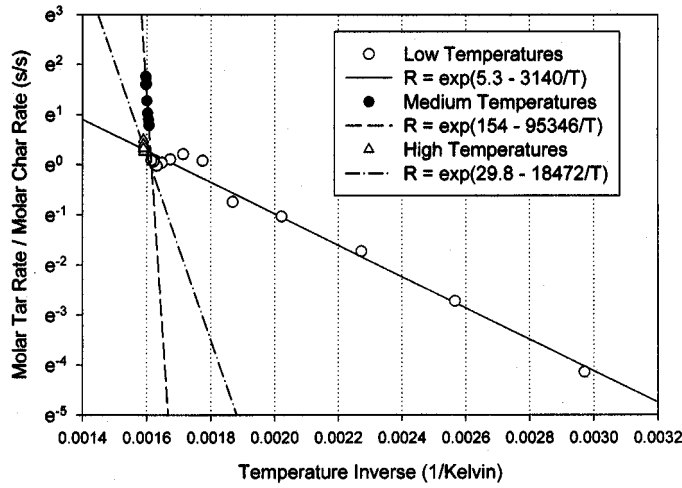


Figure 5. Kinetics correlation for molar ratio of tar to char

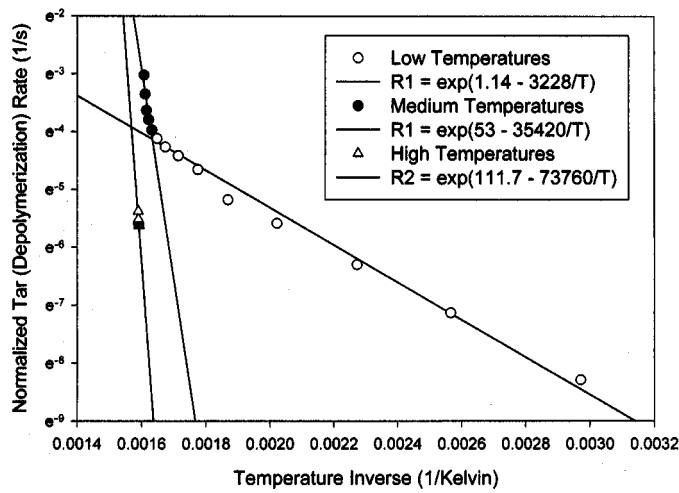


Figure 6. Kinetics correlation of normalized tar (depolymerization) rate.

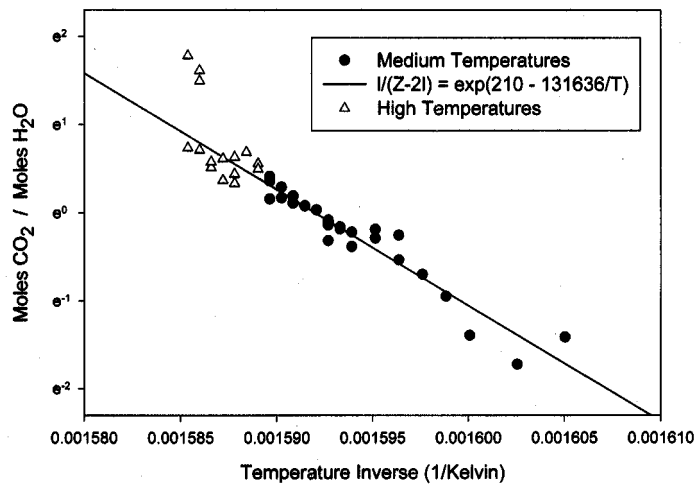


Figure 7. Kinetics correlation ratio of carbon dioxide to water vapour in volatiles.

two temperature regions involved a material (probably extractives, hemicelluloses and early lignin) composing 50% original molar fraction and the third temperature region involving the remaining 50% molar fraction of

another material (probably alpha cellulose and late lignin with a high degree of polymerization). The results for the first temperature region started out with the domination of the dehydration reactions, and as the

temperature approached 250°C the depolymerization process began to overtake the dehydration rates. The second temperature region involved a very dramatic increase in the activation energies, which we now label as the flash pyrolysis kinetics for the first material. It also involved a dramatic switch in charring reactions from dehydration to decarboxylation. This can also be visualized as the volatilization process turning about the pivot point,  $r_{o,piv} = 1.12$ ,  $c_{piv} = 3r_{o,piv}/8$ , in Fig. 4 such that  $\alpha$  rapidly changes from zero to some steady value. It is possible some other pivot point is more appropriate; however, our present objective is to reproduce the primary Pyrocat data with at least a feasible kinetics model. The high activation energies for the third temperature region seemed to imply flash pyrolysis kinetics for the second material. The results for unextracted Douglas fir are summarized by

$$l/(Z - 2l) = \exp(210 - 131636/T) \quad (31)$$

$$\dot{z}_{b,1}/\dot{z}_{c,1} = \exp(5.3 - 3140/T) + \exp(154 - 95346/T) \quad (32)$$

$$\dot{z}_{b,2}/\dot{z}_{c,2} = \exp(29.8 - 18472/T) \quad (33)$$

$$\dot{z}_{b,1}/(0.5 - z_{b,1} - z_{c,1}) = \exp(1.14 - 3228/T) + \exp(53 - 35420/T) \quad (34)$$

$$\dot{z}_{b,2}/(0.5 - z_{b,2} - z_{c,2}) = \exp(111.7 - 73760/T). \quad (35)$$

The kinetics model is now complete (cracking of tar is discussed later). The model is put into a predictive mode by using only temperature and time as the input data. Time is needed as an input because of the numerical integration for the four first-order differential equations prescribed by Eqns (32)–(35). We note that  $\alpha$  is now computed indirectly from Eqn (31) through Eqn (30) and  $\beta$  is merely the slope between the intercept point,  $(0, \mathbf{a})$ , to the pivot point,  $(r_{o,piv}, c_{piv})$ . The resulting solution is then used to evaluate the rate of volatile emission given by Eqn (25), as well as for the rates of its subcomponents as tar, water vapour and carbon dioxide. The result is shown in Fig. 8 compared with the Pyrocat data, with excellent agreement. The predicted decomposition of Eqn (25) into carbon, hydrogen and oxygen are shown as curves in Fig. 4 as

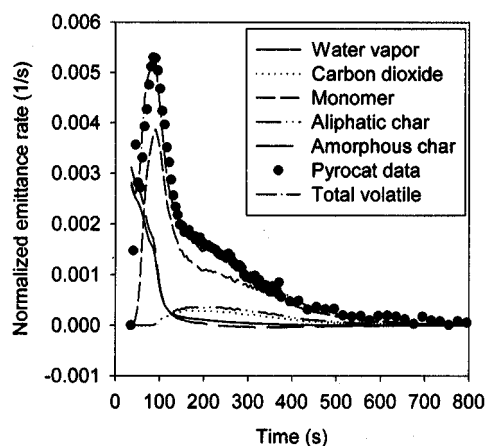


Figure 8. Modelling rates of volatile and char contents.

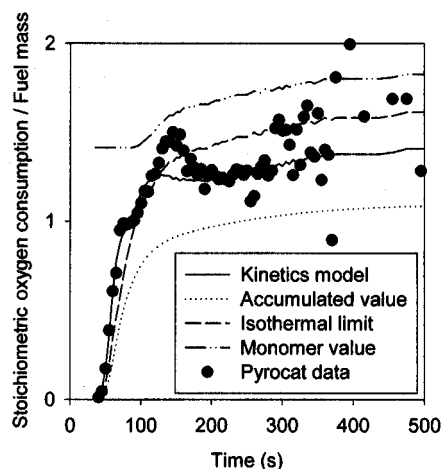


Figure 9. Modelling oxygen consumption to fuel ratio.

a function of  $r_o$  and are in good agreement with the Pyrocat data. The predicted stoichiometric oxygen consumption to fuel ratio, from rearranging Eqn (27) as  $r_o = r_{max} / \{1 + [\dot{z}_c/\dot{z}_b][44l + 18(Z - 2l)]/[12X + Y + 16Z]\}$ , is shown as the solid line in Fig. 9 and is in good agreement with the Pyrocat data.

Interesting results can be obtained by examining other aspects of the model. For example, by computing the accumulated values for predicted stoichiometric oxygen consumption to fuel ratio as a function of time, we obtain values not going any higher than unity compared with typical local values of about 1.3. This shows that the heat of combustion for volatiles as derived from bomb calorimetry data is not directly indicative of the time-dependent behaviour of the volatiles. One other predicted aspect is the isothermal limit (where the rate of temperature rise is infinite while reaching an equilibrium temperature). In this case the model predicts a lowering of  $r_o$  at low temperatures while increasing it above the nominal value at high temperatures. One therefore naturally predicts an increase for the net heat of combustion as the internal rate of temperature rise increases, as would happen when applying higher surface heat flux to the material in the cone calorimeter environment. One will also naturally deduce a higher surface temperature at ignition as the critical flux is approached because of the lowering of  $r_o$  at low temperatures. Another isothermal example is shown in Fig. 10 for the residual mass fraction plotted as function of temperature. The predicted curve for the nominal case is in good agreement with the Pyrocat data. The isothermal curve is shown as the dashed line. Thus at low temperatures the dehydration will achieve char mass fraction of around 50%, where at around 300°C the char mass fraction begins to rapidly decrease and possibly vanish by 400°C. The model is also in qualitative agreement with data that showed the residue mass fraction at the end time decreases with the increase in the temperature rise rate.<sup>27</sup> The robustness of the model is suggested by other data in which complete charring was obtained under nominal conditions (heated in a furnace).<sup>10,21</sup> The vanishing of char at very high temperature is also in qualitative agreement with the flash pyrolysis data. As final, yet crucial data for this

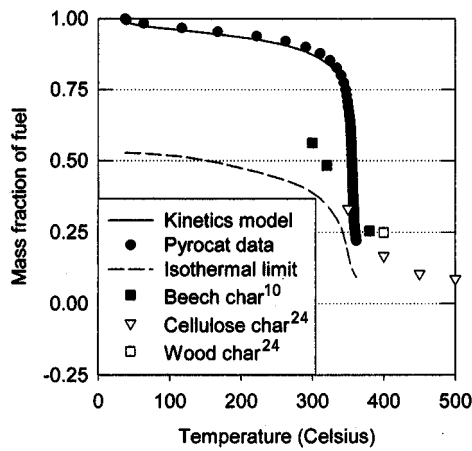


Figure 10. Modelling residual mass fraction.

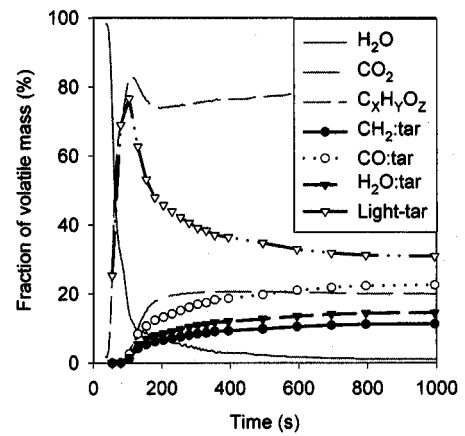


Figure 12. Modelling thermal cracking of heavy tar.

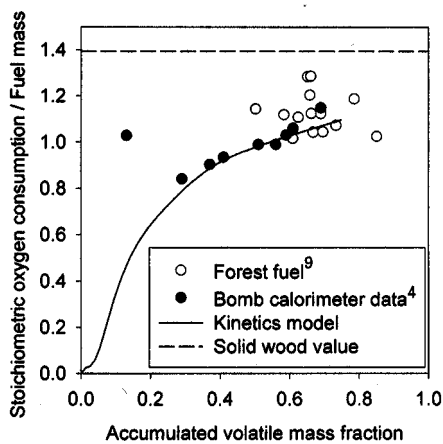
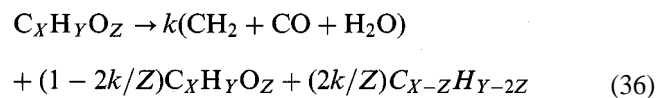


Figure 11. Accumulated parameters for Douglas-fir.

paper. Parker and LeVan<sup>4</sup> describe results from the bomb calorimeter data of unextracted Douglas-fir wood used in the Pyrocat tests. Their data were not used in Fig. 1, because it was reported as gross heat of combustion varying with residue mass fraction and without the corresponding ultimate analysis. Fig. 11 shows the predicted accumulated  $r_o$  from Fig. 9 plotted as a function of the accumulated volatile fraction using the predicted residue mass fraction from Fig. 10. The bomb calorimeter data were converted by first applying Eqn (16) to obtain the net heat of combustion and dividing by 13.23 to obtain ‘experimental’  $r_o$  for the residues. The ‘experimental’  $r_o$  of the accumulated volatiles were then derived using Eqn (3) and the measured residue mass fraction. Unity minus the measured residue mass fraction is the accumulated volatile mass fraction. The result is the solid circle data in Fig. 11 in good agreement with the predicted results. The model prediction is comparable to the forest fuel data by Susott and others shown by open circles. Despite the various shortcomings of the Pyrocat apparatus, oxygen bomb calorimeter, and the mechanistic kinetics model, this analysis shows the net heat of combustion correlation as given by Eqn (5) is indeed applicable to instantaneous wood volatiles, while the data from the oxygen bomb calorimeter only pertains to accumulated properties.

To examine tar cracking we first plotted the predicted mass fractions of the water vapour, carbon dioxide and monomer, as a function of time in Fig. 12. From Fig. 8 we observed that the char portions of the residue also follow the same trends as the water vapour from dehydration and carbon dioxide from the decarboxylation. The rising of the monomer (tar) to a nearly constant level with a corresponding decreasing water vapour/carbon dioxide (char formation) is quite similar to a plot shown by Shafizadeh<sup>28</sup> for vacuum pyrolysis of cellulose at 375°C. The nearly constant values of the monomer mass fraction and elemental compositions are consistent with nearly constant net heat of combustion after 100 s as implied in Fig. 9. Shafizadeh suggested in other publications<sup>21</sup> that the atmospheric pressure promotes interaction among the primary volatile products to cause a further breakdown of the tar. Therefore, we suggest a possible thermal cracking of the evaporated monomer as,



$$\frac{2k/Z}{1 - 2k/Z} = \exp(210 - 131636/T) \quad (37)$$

where the kinetic constants were simply borrowed from Eqn (31) as it had the highest activation energy. Suppose for simplicity the monomers are glucose,  $C_6H_{12}O_6$ , and they had cracked completely into water vapour, carbon monoxide and simple aliphatic hydrocarbons. Then according to Eqns (5) and (9) the cracked gas mixture has an increase in net heat of combustion of 0.74 kJ/g, or ~ 5% increase over that of the original glucose monomer. On the other hand, if the glucose had cracked completely into methane and carbon dioxide instead, then the cracked gas mixture would have a heat of combustion decrease of 0.77 kJ/g, or ~ 5% decrease under that of the original glucose. The previous two examples are seen as extreme thermal cracking that result in a maximum amount of, yet quite small, changes in their net heat of combustion. The mass fraction predictions for the thermal cracking products of

Eqns (36) and (37) are shown in Fig. 12. One observes that carbon monoxide and carbon dioxide are about equal at 20% and the total hydrocarbons value is half that at 10% at the end of the test. The lighter tar at first increases to a peak and then is monotonically decreasing, while water vapour from the cracking is monotonically increasing with time. If we were working with a thick wood specimen, the water vapour generated from dehydration at the lower temperature region within the wood would likely dilute the thermally cracked volatiles from the high temperature region within the char layer. One would get a profile for the volatile products similar to that measured by Ohlemiller and others<sup>29</sup> for a thick dried white pine exposed to an irradiance of 40kW/m<sup>2</sup> in a flowing nitrogen environment.

---

## CONCLUSION

---

In this paper we reexamined various data published on the pyrolysis of wood for the purpose of understanding the results of cone calorimeter tests on wood-related products. Based on oxygen bomb calorimeter data and ultimate analysis of various biomass and waste materials (including their charred residues), we derived a net heat of combustion correlation given by Eqn (5). This correlation also extends to the bomb calorimeter data pertaining to wood structural content as well as to instantaneous wood volatile content, regardless of the level of thermal degradation of evaporated monomers or amount of fire-retardant treatment within the wood. The exemplary unification of disparate sources of bomb calorimeter data for forest and wood products (and common plastic products), even dating back several decades, has now been achieved in a single correlation. However, the need for new data from the combustion bomb calorimeter tests and ultimate analysis for some recent wood product developments still exist. One may find that of the various fire retardant treatments in various wood products, a few may present exceptions to the net heat of combustion correlation. This database would then be essential for addressing the needs for performance-based codes and of engineering for fire safety.

In this paper, a revision to processing of cone calorimeter data is suggested for better accuracy on the various heat of combustions. A method has been described to obtain carbon, hydrogen and oxygen contents of the volatiles from existing cone calorimeter data if it can be assumed the volatiles contain only carbon, hydrogen and oxygen. In addition, data acquisition in the modern cone calorimeter can be reconfigured to achieve high fidelity in the various recorded signals. With these data the instantaneous and stoichiometric values for gross and net heat of combustions for wood volatiles can be calculated. A formula was provided for the reduction of heat of combustion due to incomplete oxidation reactions that produce carbon monoxide and soot. This incomplete net heat of combustion tends to provide overall values in agreement with the effective heat of combustion specified in the cone calorimeter standard.

Because of the special effect that boundary conditions (such as surface heat flux, heavy backing, or flame dimensions) have on the heat-release, smoke and soot rates<sup>3,5</sup> of wood specimens, there are difficulties in extrapolating the measured properties to full-scale fires. The mechanistic kinetic analysis in this paper for predicting volatilization rate, net heat of combustion and various elemental mass fractions as functions of time provided some insights to these difficulties. For example, if the rate of temperature rise is low (as with low surface heat fluxes or heavy backing) then dehydrations occur relatively more than do 'tar' evaporations in the wood structure. This means the heat of combustion will be lower, conversion to char will be higher, and volatile rates will be lower. In the cone calorimeter tests these effects would mean an increase in surface temperature at ignition and a reduction in the first and second peak heat release rate on a thick specimen.

The novel kinetics analysis provided in this paper only needed a single, but very well performed, Pyrocat test of a thin specimen. Certain other data were shown to indicate qualitatively the robustness of the model. A quantitative assessment of the model's robustness should include comparison with test runs of specimens exposed to thickness, heat flux and backing variations. A very thin specimen (1 mm or less) in the cone calorimeter test should respond similarly as shown in Figs 4 and 8 for the Pyrocat apparatus, but more rapidly and with less temperature gradient within the specimen during radiant heat exposure. However, to better emulate the Pyrocat's complete combustion, an auxiliary methane burner in the volatile stream would be needed to ensure that all the tar and hydrocarbons are combusted in the modified cone calorimeter protocol. Further refinements in the mechanistic kinetics model can be obtained from a high fidelity data as well as a more thorough characterization of primary monomers during their evaporation and thermal cracking process.

---

## NOMENCLATURE

---

<i>a</i>	Ash mass fraction
<i>c</i>	Carbon mass fraction
<i>C</i>	Carbon symbol
<i>h</i>	Hydrogen mass fraction
<b>D</b> <i>h<sub>c</sub></i>	Heat of combustion (kJ/g)
<i>k</i>	Molar fraction of tarring monomers to gas
<i>l</i>	Molar fraction of charring monomers to CO <sub>2</sub>
<i>ṁ</i>	Mass flow rate (g/s)
<i>o</i>	Oxygen mass fraction
<i>O</i>	Oxygen symbol
<i>r<sub>o</sub></i>	O consumption mass/fuel mass
<i>s</i>	Sulphur mass fraction
<i>S</i>	Sulphur symbol
<i>T</i>	Absolute temperature (Kelvin)
<i>X</i>	Number of C atoms in monomer
<i>y</i>	Mass fraction of original sample
<i>Y</i>	Number of H atoms in monomer
<i>z</i>	fraction of original monomers
<i>Z</i>	Number of O atoms in monomer
<b>a</b>	Intercept in Equation (14)
<b>β</b>	<i>r<sub>o</sub></i> coefficient in Equation (14)

## REFERENCES

1. ASTM E 1354-92. *Standard Test Method for Heat and Visible Smoke Release Rates for Materials and Products using an Oxygen Consumption Calorimeter*. American Society for Testing and Materials: Philadelphia, PA, 1992.
2. Atreya A. *Pyrolysis, Ignition, and Fire Spread on Horizontal Surfaces of Wood*, 1983, Ph.D. Dissertation. Division of Applied Sciences, Harvard University: Cambridge, MA.
3. Dietenberger M. *Proc. Int. Conf. on Fire Safety*. Product Safety Corporation: Sissonville, W. VA, 1999; **28**: 62-73.
4. Parker W, LeVan S. *Wood Fiber Sci.* 1989; **21**: 289-305.
5. Dietenberger M, Grexa O. *Proc. 4th Int. Sci. Conf. on Wood & Fire Safety*. Technical University of Zvolen: Slovak Republic, 2000; Pt. 1, 45-55.
6. ASTM E 1591-94. *Standard Guide for Obtaining Data for Deterministic Fire Models*. American Society for Testing and Materials: Philadelphia, PA, 1999.
7. ASTM D 3286-91a. *Standard Test Method for Gross Calorific Value of Coal and Coke by the Isoperibol Bomb Calorimeter*. American Society for Testing and Materials: Philadelphia, PA, 1991.
8. Hugget C. *Fire Mater* 1980; **4**: 61-65.
9. Susott R, DeGroot R, Shafizadeh F. *J. Fire Flamm.* 1975; **6**: 311-324.
10. Roberts AF. *Combust. Flame* 1964; **8**: 345-346.
11. Chen Y, Frendi S, Tewari S, Sibulkin M. *Combust. Flame* 1991; **84**: 121-140.
12. Babrauskas V. *Heat Release in Fires*. Elsevier Science: New York, 1992; 207-223.
13. Schlesinger M. *Marks Standard Handbook for Mechanical Engineers*, McGraw-Hill: New York, 1996; 7.2-7.16.
14. Tillman D. *Wood as an Energy Resource*. Academic Press: New York, 1978; 65-87.
15. Graboski M, Bain R. *Biomass Gasification: Principles and Technology*, Noyes Data Corporation: New Jersey, 1981; 41-71.
16. Weissinger A, Obernberger I. *Fourth Biomass Conference of the Americas*. Elsevier Science: Oakland, CA, 1999; **2**: 1417-1424.
17. Reed TB. *Thermodynamic Data for Biomass Materials and Waste Components*, Appendix A, Domalski ES, Jobe T, Milne TA (eds). American Society of Mechanical Engineers: New York, 1987.
18. Browne FL, Brenden JJ. *Heat of Combustion of the Volatile Pyrolysis Products of Fire-retardant-treated Ponderosa Pine*. Research Paper FPL 19, USDA Forest Service. Forest Products Laboratory: Madison, Wisconsin, 1964.
19. White RH. *Wood Fiber Sci.* 1987; **19**: 446-452.
20. Rothermal RC. *Thermal Uses and Properties of Carbohydrates and Lignins*, Shafizadeh F, Sarkanen K, Tillman D (eds). Academic Press: New York, 1976; 245-259.
21. Shafizadeh F. *The Chemistry of Solid Wood*. R Rowell (ed.). ACS Symposium Series 207. American Chemical Society: Washington, DC, 1984; 489-529.
22. Buchanan, MA. *The Chemistry of Wood*. Browning B, (ed.). John Wiley & Sons, Inc., reprint by Robert E. Krieger Publishing Co: New York, 1975; 314-367.
23. Fangrat J, Hasemi Y, Yoshida M, Kikuchi S. *Fire Mat.* 1998; **22**: 1-6.
24. Antal MJ, Varhegyi G. *Ind. Eng. Chem. Res.* 1995; **34**: 703-717.
25. White RH, Dietenberger MA. *Encyclopedia of Materials: Science and Technology*. Elsevier: New York, 2001; 9712-9716.
26. Broido A. *Thermal Uses and Properties of Carbohydrates & Lignins*. Shafizadeh F, Sarkanen KV, Tillman DA (eds). Academic Press: New York, 1976; 19-35.
27. Helt JE, Agrawl RK. *Pyrolysis Oils from Biomass*. Soltes EJ Milne TA (eds). ACS Symposium Series 376. American Chemical Society: Washington, DC, 1988; 79-91.
28. Shafizadeh F. *TAPPI Forest Biology Wood Chemistry Conference*. TAPPI: Atlantic, GA, 1977; 191-199.
29. Ohlemiller TJ, Kashiwagi T, Werner K. *Combust. Flame.* 1987; **69**: 155-170.